JOURNAL OF GEOPHYSICAL RESEARCH, VOL. 112, F03021, doi:10.1029/2006JF000725, 2007

Evidence for late Pleistocene thinning of Siple Dome, West Antarctica

S. F. Price,[1,2] H. Conway,[1] and E. D. Waddington[1]

Received 16 November 2006; revised 24 February 2007; accepted 14 May 2007; published 21 August 2007.

[1] We use a two-dimensional, full-stress, thermomechanical flow band model to investigate late Pleistocene and Holocene histories of ice thickness and ice flow at Siple Dome in West Antarctica. Measurements obtained from an ice core and borehole near the ice divide and measurements of radar-detected internal stratigraphy are used as targets for modeling. Models that account for the climate history (accumulation rate and temperature) alone yield a poor match to observations; histories of ice dynamics (ice thickness, ice divide location, and ice flow enhancement) also need to be included. Our favored model includes 350 m of thinning at Siple Dome between 15,000 and 14,000 years ago, onset of divide flow 3000 years ago, ongoing divide migration starting 2500 years ago, and evolution of ice fabric over the past 30,000 years. The timing of thinning is earlier than that inferred from geologic evidence from the margins but is coincident with a 20 m rise in global sea level about 14,500 years ago (meltwater pulse 1A). This opens the possibility that thinning was a result of increased activity of the ice streams in the late Pleistocene, forced by meltwater pulse 1A. The contribution to meltwater pulse 1A as a result of this thinning was likely small.

Citation: Price, S. F., H. Conway, and E. D. Waddington (2007), Evidence for late Pleistocene thinning of Siple Dome, West Antarctica, *J. Geophys. Res.*, *112*, F03021, doi:10.1029/2006JF000725.

1. Introduction

[2] Ice thickness in West Antarctica during the last glacial maximum (LGM) and the timing of deglaciation are poorly known, and yet this information is key for understanding how ice streams influence the stability of the ice sheet, and for evaluating the contributions of the ice sheet to global sea level change. Recent reconstructions of the Ross Sea sector of the West Antarctic Ice Sheet that are based on moraine limits [*Denton et al.*, 1991] and glacial-marine deposits [*Anderson et al.*, 2002] observed around the margins, point to a much thicker ice sheet during the LGM [*Denton and Hughes*, 2002; *Huybrechts*, 2002]. Implicit in these two reconstructions is that the lengths of the fast-flowing ice streams that control discharge from West Antarctica remain constant; that is their onset regions were farther west during the LGM and the ice streams have migrated inland as the grounding line retreated.

[3] However, numerical experiments with a thermomechanical model indicate that although the ice streams may have slowed during the LGM, they probably did not stagnate [*Parizek et al.*, 2003]; *Parizek and Alley* [2004] inferred thickening of only ~100 m at Siple Dome (SDM in Figure 1) during the LGM. *Waddington et al.* [2005] also inferred low surface elevations in the central Ross Sea during the LGM. They used a time-dependent, one-dimensional ice flow model to investigate combinations of ice thickness, divide position, and accumulation rate histories that matched the observed age-depth relationship at Siple Dome. Combinations with physically unrealistic accumulation rate histories were rejected and they concluded that Siple Dome was at most 200–400 m thicker during the LGM [*Waddington et al.*, 2005].

[4] Improved understanding of the timing of deglaciation is needed to establish the response of the ice sheet to past and possible future environmental change. *Steig et al.* [2001] reinterpreted the stable isotope record from the Byrd ice core (NBY in Figure 1) and suggested that the ice sheet there has thinned about 200 m in the past 10 ka. *Conway et al.* [1999] used geologic evidence from the Scott Coast and the Transantarctic Mountains and glaciological models and observations from Roosevelt Island (RI, Figure 1) to map Holocene grounding-line retreat in the Ross Sea Embayment. They showed that deglaciation was under way 8000 years before present (8 ka BP) but the data were not sufficient to resolve whether grounding-line retreat is continuing today. *Stone et al.* [2003] measured surface exposure ages of glacial deposits in the Ford Ranges (FR, Figure 1) and showed that deglaciation of western Marie Byrd Land that started about 10 ka BP is likely ongoing.

[5] Here we investigate histories of ice thickness and deglaciation in the central Ross Sea Embayment using observations from Siple Dome and a two-dimensional, thermomechanical flow band model [*Price et al.*, 2007].

[1] Department of Earth and Space Sciences, University of Washington, Seattle, Washington, USA.
[2] Now at Bristol Glaciology Centre, School of Geographical Sciences, University of Bristol, Bristol, UK.

0148-0227/07/2006JF000725$09.00

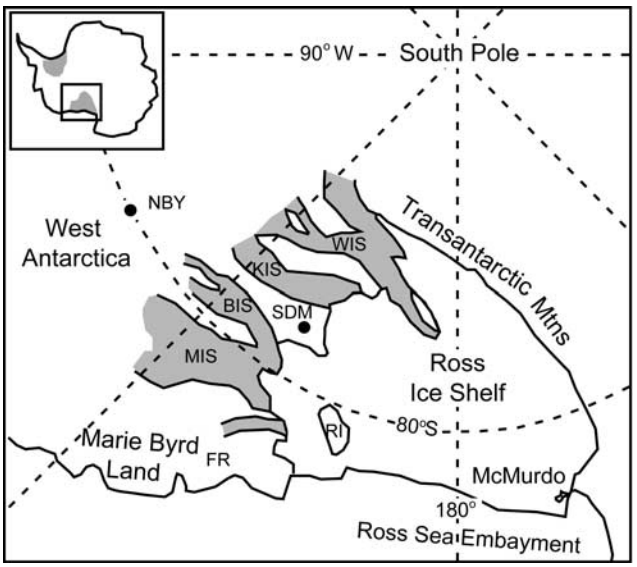

Figure 1. Siple Dome location map. Siple Dome (SDM); Roosevelt Island (RI); Byrd Station (NBY); Ford Ranges (FR); and Whillans (WIS), Kamb (KIS), Bindschadler (BIS), and MacAyeal (MIS) ice streams.

Data sources and previous work at Siple Dome, used to constrain the modeling, are discussed below.

2. Data Sources and Previous Work

[6] A 1004-m ice core was recovered between 1997 and 1999 from a site 0.5 km south of the present divide location at Siple Dome. Relevant observations and analyses include:

[7] 1. Age-depth relationship. The core was dated by counting annual layers to a depth of 515 m [*Taylor et al.*, 2005] and by correlating measurements of occluded CH_4 with measurements from the well-dated GISPII ice core from Greenland [*Brook et al.*, 2005].

[8] 2. Temperature profiles. *Engelhardt* [2004] logged temperature profiles down several boreholes in the vicinity of Siple Dome. Measurements and calculations indicate the geothermal flux is 0.071 Wm^{-2} [*Engelhardt*, 2004; G. Clow, personal communication, 2004].

[9] 3. Stable isotope profile. A. Schilla (personal communication, 2007) used measurements of stable isotopes and the age-depth relationship to infer a surface temperature history (see also Appendix A).

[10] 4. Bubble-number density. *Spencer* [2005] used a model for firn compaction and grain growth, a temperature history from the stable isotopes, and measurements of bubble-number densities along the core to derive an accumulation rate history for the past 30 ka.

[11] 5. Ice thickness and internal stratigraphy. *Jacobel et al.* [1996] used radio echo sounding methods to measure ice thickness and internal layering across the ice divide. Bedrock elevations were derived from measurements of surface elevation and ice thickness [*Raymond et al.*, 1995]. *Nereson et al.* [1998a, 1998b, 2000] interpreted the internal layers using kinematic ice flow models. They concluded that (1) Siple Dome has been an elevated feature for most of the Holocene; (2) the ice divide has been migrating northward for the past several thousand years at a rate of $\sim$0.5 ma^{-1}; and (3) ice thickness has not changed significantly over the past 2 ka. They could not rule out the possibility of thickness changes prior to 2 ka BP.

[12] 6. Ice fabric and texture. *DiPrinzio et al.* [2005] measured ice fabric and texture along the ice core. G. Lamorey (personal communication, 2004) measured sonic velocities down the borehole.

[13] 7. Vertical velocity. Direct measurements of submergence velocities [*Hamilton*, 2002], and depth profiles of the vertical strain rate [*Hawley et al.*, 2004; *Zumberge et al.*, 2002], all indicate that the divide region is now near steady state, but the flanks are thinning 0.02–0.05 ma^{-1}.

3. Modeling Approach

[14] Our approach is similar to that used by *Waddington et al.* [2005] but in addition to the age-depth relationship we also use borehole temperature measurements and the pattern of radar-detected isochrones (including the surface topography) as targets for modeling. The full-stress, flow band model [*Price et al.*, 2007] solves the two-dimensional momentum balance equations (i.e., plane strain) and the two-dimensional, advective-diffusive heat equation using the finite volume method. When solving the momentum equations, we make the simplifying assumption that $\rho\ (x, z, t) = \rho_{ice}$. The model domain for the momentum calculation spans 20 km on either side of the divide. When solving the heat equation in firn, we follow methods given by *Paterson* [1994]. The model domain for the heat calculation includes a 1.5-km layer of bedrock beneath the ice. Bedrock elevations are held constant; isostatic rebound is not taken into account. The geothermal flux (0.071 Wm^{-2}) is assumed constant throughout each model run.

[15] We specify a climate history (accumulation rate and surface temperature) for the past 120 ka (shown in Figure 2). The accumulation rate history for the past 30 ka comes from *Spencer* [2005]. Prior to that time we extrapolate the accumulation rate linearly back in time to a value that is the same as today (0.12 m a^{-1}) (we assume that accumulation during the last interglacial was the same as today) (Figure 2a). The surface temperature history (Figure 2b) comes from A. Schilla (personal communication, 2007). We use this climate history and run forward models to examine the response to different prescribed histories of ice dynamics. Model results at the end of each 120 ka run are compared with measurements of the age-depth relationship, the temperature profile, and radar detected isochrones (including the present-day surface topography). Below we discuss how histories of divide location, ice thickness, ice fabric, and divide scouring by wind affect properties observed in the ice sheet today, and how these histories are treated in the model.

3.1. History of Divide Location

[16] Vertical velocities at mid depths beneath a stable ice divide are less than those on the flanks [*Raymond*, 1983]; the age at a given depth beneath a divide is older than beneath a flank site of similar thickness. Further, relatively low vertical velocities at a divide cause the ice there to be warm compared with the flanks [*Paterson and Waddington*, 1986; *Dahl-Jensen*, 1989] and result in a distinct upwarping

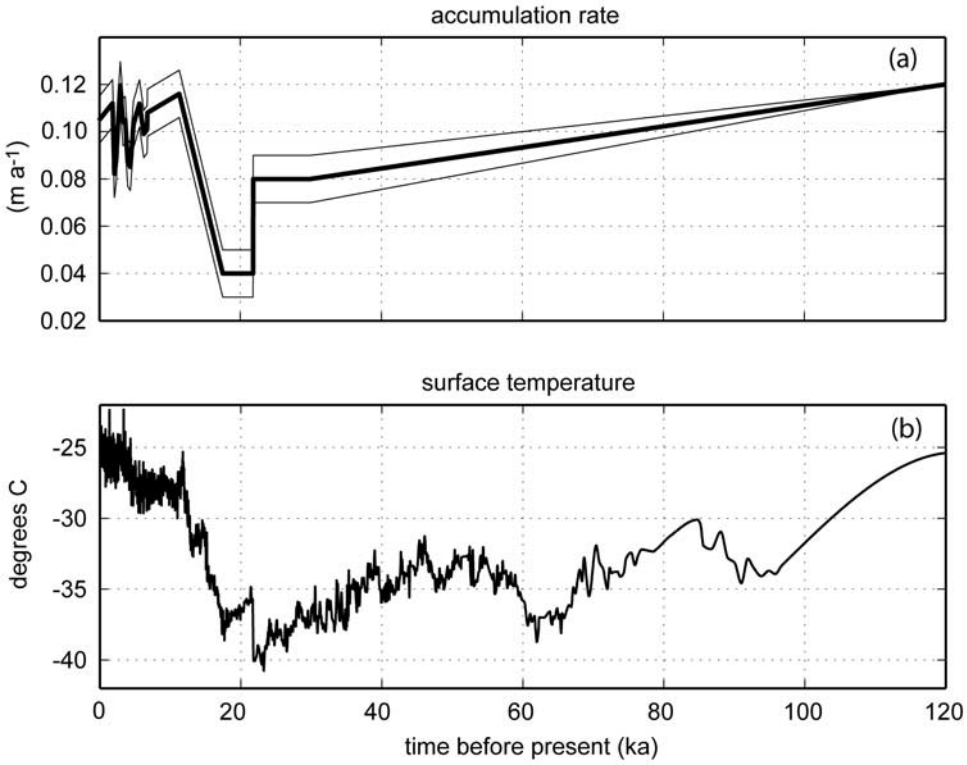

Figure 2. Climate histories for Siple Dome. (a) Surface accumulation rate history back to 30 ka BP from *Spencer* [2005]. Prior to that time, the history is extrapolated back linearly to 0.12 ma^{-1} 120 ka BP. The thin curves denote the uncertainty envelope discussed in Figure 13. (b) Surface temperature history from A. Schilla (personal communication, 2007).

of internal layers (a ''Raymond bump'') beneath a flow divide. Divide migration causes the velocity field to change from divide-like flow to flank-like flow; beneath a migrating divide the age will be younger and the temperature profile will be cooler than beneath a stationary divide. Divide migration also ''smears'' an existing divide bump laterally, decreasing its amplitude and tilting its axis in the direction of migration [*Nereson and Waddington*, 2002].

[17] To quantify the effects of divide proximity on internal layer shape, we measure the bump amplitude as a function of depth; for a given layer, the bump amplitude is calculated relative to a datum that is generated from a spline fit to the layer shape outside the region affected by divide flow. With increasing time after the onset of divide flow, the maximum amplitude of the bump increases, and the location of that maximum occurs closer to the bed.

[18] Particles that were in close proximity at the surface are separated by diverging flow, which makes tracking of deep (old) layers in the model difficult. This is especially true for cases of a migrating divide; particles needed to describe deep layer shapes may be advected (horizontally) out of the domain before they reach a significant depth. Here, we examine just two of many possible transitions: (1) a flank that becomes a divide instantaneously, and (2) a divide that has migrated recently relative to the present (in which case horizontal advection has only a minor effect on very shallow layers). Details of our treatment of these two transitions are given in Appendix B.

3.2. Ice Thickness History

[19] The ice thickness history influences the depth-age relationship, the pattern of internal stratigraphy, and the temperature profile observed in an ice sheet today. In an ice sheet that has thinned, an annual layer at a given depth is older than a layer at the same depth in an ice sheet that has not thinned: the layer in the ice sheet that has thinned has undergone more strain thinning to get to the same depth (assuming that both ice sheets have the same accumulation rate and present ice thickness). Thinning also has the effect of increasing both the bump amplitude and the depth of its maximum because the difference between flank and divide flow regimes is enhanced in a thinning ice sheet. The temperature profile observed in an ice sheet today depends on the profile prior to thinning, as well as on the magnitude, duration, and timing of thinning. Other things being equal, a thick ice sheet will have colder surface temperatures (assuming a standard atmospheric lapse rate) but thick ice is more insulating. Although the surface may be colder, the basal temperature may be warmer than that beneath a thin ice sheet. During thinning, cold surface ice is advected to depth faster than in an ice sheet in steady state. Either a large thickness change over a long period of time or a small thickness change over a short period of time could produce a temperature profile that is cool at depth relative to that for an ice sheet in steady state.

[20] We assume that Siple Dome was at least as thick and likely thicker than today during the last glacial period. For

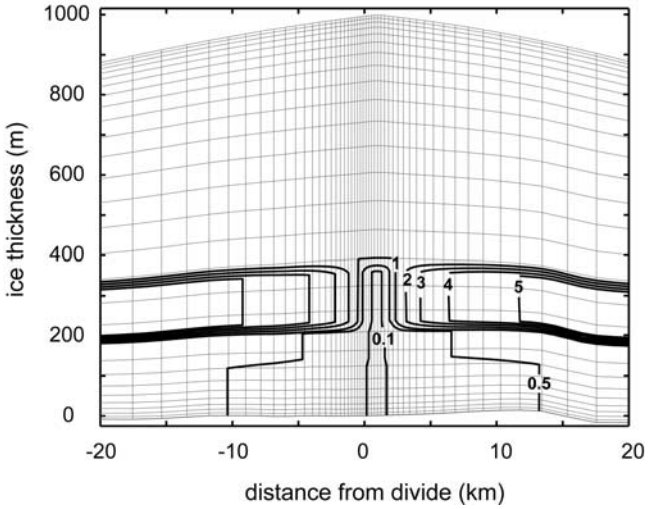

Figure 3. Map of favored value for the enhancement factor, E, across Siple Dome today.

most of that time, we assume a quasi-steady state in which accumulation integrated over the surface is balanced by ice flux at the lateral boundaries. That is, we hold the volume of the model domain constant and allow the surface shape to evolve with time. To force thinning at a specified rate and time, we increase the ice flux at the lateral boundaries relative to the balance flux. Similarly, divide migration is forced by changing the boundary fluxes asymmetrically. Changes in flux and thickness initiated at the margins propagate up to the divide and the surface topography adjusts to a new steady state that is consistent with the new thickness and climate. Under present-day conditions, the time required for the surface of Siple Dome to adjust to thickness changes at the margins is about 700 years [*Nereson et al.*, 1998a]. Changes that occurred more than 700 years ago no longer affect the surface shape today.

3.3. Evolution of Ice Fabric and Flow Enhancement

[21] While ice fabric and texture exert a strong control on the mechanical properties of ice, a rigorous treatment of their spatial and temporal evolution is beyond the scope of this work. Here, we parameterize their mechanical effects by scaling the flow law for ice by an enhancement factor, E, that varies in space and time: stiff ice is represented by $E < 1$, and soft ice by $E > 1$. In general, a single value for E is not appropriate for approximating the mechanical effects of an oriented c axis fabric, which makes ice simultaneously soft to horizontal shear and stiff to vertical compression. To get around this restriction, we take advantage of the fact that, near a flow divide, vertical compression (and longitudinal extension) dominates over horizontal shear and, away from a divide, the opposite holds true. This allows us to adapt the method of *Wang and Warner* [1999], which calculates a value for E in various states of combined compression and shear: for flow only in vertical compression, $E = E_C$, and for flow only in horizontal shear $E = E_S$. For ice undergoing a combination of compression and shear, $E_C < E < E_S$. We adapt the *Wang and Warner* [1999] method so that, when a c axis fabric is present, we calculate a stiff value ($E < 1$) for ice near the divide and a soft value ($E > 1$) for ice on the flanks. At transitional locations, E varies smoothly according to the relative contribution of vertical compression to the total strain.

[22] Measurements along the Siple Dome ice core [*Diprinzio et al.*, 2005] and a sonic log down the borehole (G. Lamorey, personal communication, 2004) have been used to characterize the present-day ice fabric and texture. The lowest 200 m consists of large interlocking ice crystals; the fabric and texture indicate recrystallization [*Diprinzio et al.*, 2005]. Between about 200 and 300 m above the bed, grains are small and the c axis fabric is tightly oriented about the vertical. Fabric and texture in the upper section of the ice column (more than 300 m above the bed) show some evidence of oriented fabric and recrystallization, but are not so pronounced as in the lower layers.

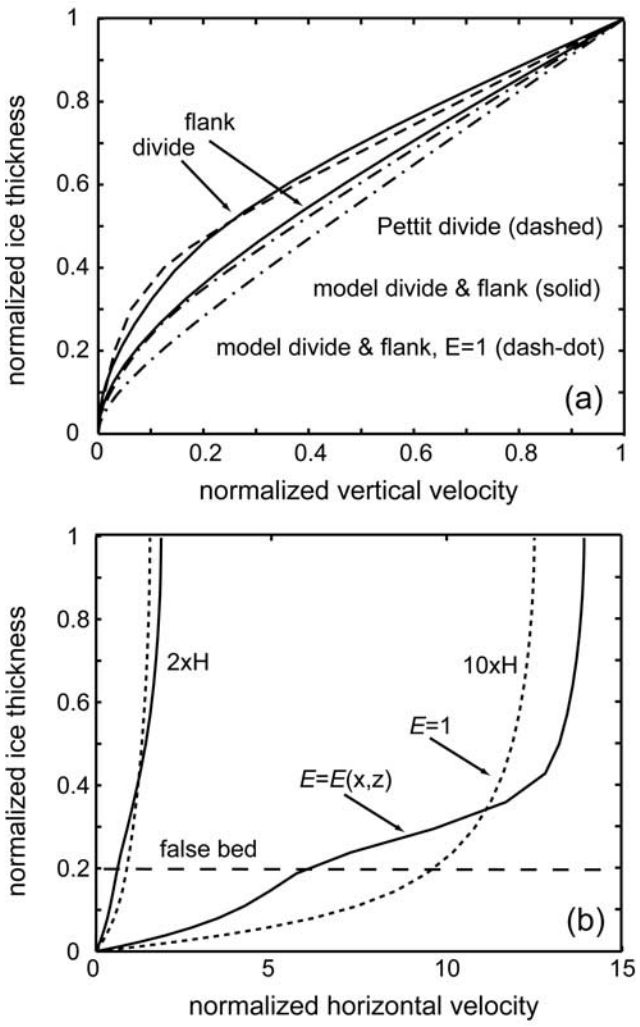

Figure 4. Present-day velocity shape functions at Siple Dome. Velocities are normalized by the present-day surface accumulation rate. (a) Model vertical velocity shape functions at the divide and flank for favored values of E shown in Figure 3 (solid curves), for $E = 1$ everywhere (dash-dotted curves), and from *Pettit* [2003] (dashed curves). (b) Model horizontal velocity shape functions at horizontal distances of $2H$ and $10H$ from the divide (H is the ice thickness) for E with favored values shown in Figure 3 (solid curves) and $E = 1$ everywhere (dashed curves).

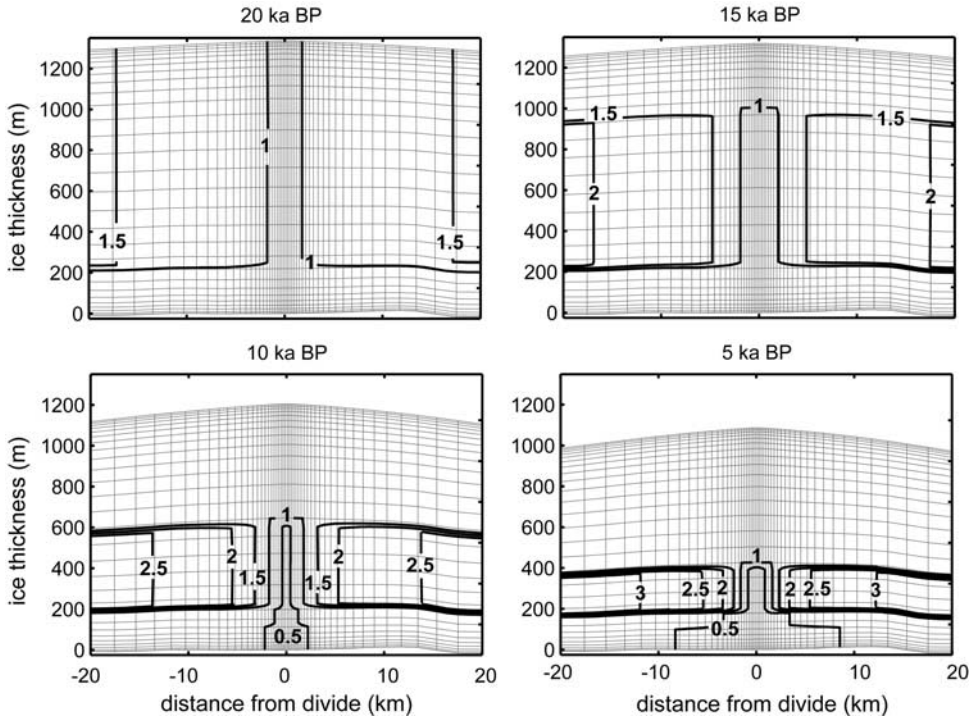

Figure 5. Prescribed value of flow enhancement across Siple Dome at four times subsequent to its initiation at 30 ka BP. The present-day enhancement field is shown in Figure 3.

[23] We assume that the upper section of the ice column (300 m above the bed to the surface) is "normal" and assign $E = 1$. Relative to isotropic ice, the ice from the "lowest layer" (0 to 200 m above the bed) is stiff. The "mid layer" (200 to 300 m above the bed) is stiff to vertical compression, and soft to horizontal shear. This stratigraphic sequence effectively causes a "false bed" [*Pettit*, 2003]; the majority of deformation in the ice column takes place above the lower layer. Figure 3 shows our favored distribution of E values across Siple Dome today; values for E_C and E_S were chosen so that our vertical velocity shape function at the divide matches that derived from a steady state model that explicitly accounts for the mechanical effects of the observed ice fabric and texture [*Pettit*, 2003]. Figure 4a shows vertical velocity shape functions from *Pettit* [2003], our favored approximation derived from Figure 3, and the case for $E = 1$ everywhere. Figure 4b shows horizontal velocity shape functions at locations $2\times$ and $10\times$ the ice thickness away from the divide. Away from the divide region we choose values for E_C and E_S so that the modeled present-day surface shape matches the observations.

[24] Details of the evolution of ice fabric and flow enhancement are not known. We assume that oriented fabric initially developed in ice age ice. Ongoing strain strengthened the fabric until it was reset by dynamic recrystallization deep in the ice column where temperatures are warmer than $-10°$C. Accordingly, the evolution of the flow law enhancement factor E is modeled using the following assumptions:

[25] 1. No significant flow enhancement ($E = 1$) prior to 30 ka BP. Starting at 30 ka BP, flow enhancement strengthens over time; E_C and E_S change linearly from a value of unity to their favored present-day values.

[26] 2. When $E \neq 1$, the lower $\sim$20% of the ice column always consists of recrystallized ice. This assumption is reasonable because model results for Siple Dome indicate that the $-10°$C isotherm is always about $0.2H$ regardless of the ice thickness H.

[27] 3. The transition from ice age ice occurred 18 ka BP (this timing comes from interpretation of the age-depth relationship and the stable isotope profile) and for ice younger than 18 ka BP we set $E = 1$. Ice older than 18 ka BP is forced to evolve through time so that the present-day values for E are consistent with those shown in Figure 3.

[28] Figure 5 shows maps of our favored distribution of flow enhancement across Siple Dome for four times subsequent to its initiation 30 ka BP.

3.4. History of Divide Scouring

[29] Spatial variations in accumulation affect the vertical velocity field, which affects the annual layer thickness, the age-depth relationship, and the temperature profile; localized and persistent wind scouring at a divide reduces accumulation and causes near-surface isochrones to appear upwarped [*Vaughan et al.*, 1999]. To simulate the effects of wind scouring, we follow *Nereson and Waddington* [2002]; the reduction in accumulation near the divide is represented by one cycle of a cosine bell curve centered on the divide. The favored scouring rate at the divide (the amplitude of the cosine bell curve) is the one that best fits the observed bump amplitude profile.

4. Model Results

[30] We have run numerous forward models using the climate history specified in Figure 2 and different histories of ice dynamics. Figure 6 shows a reference model in which

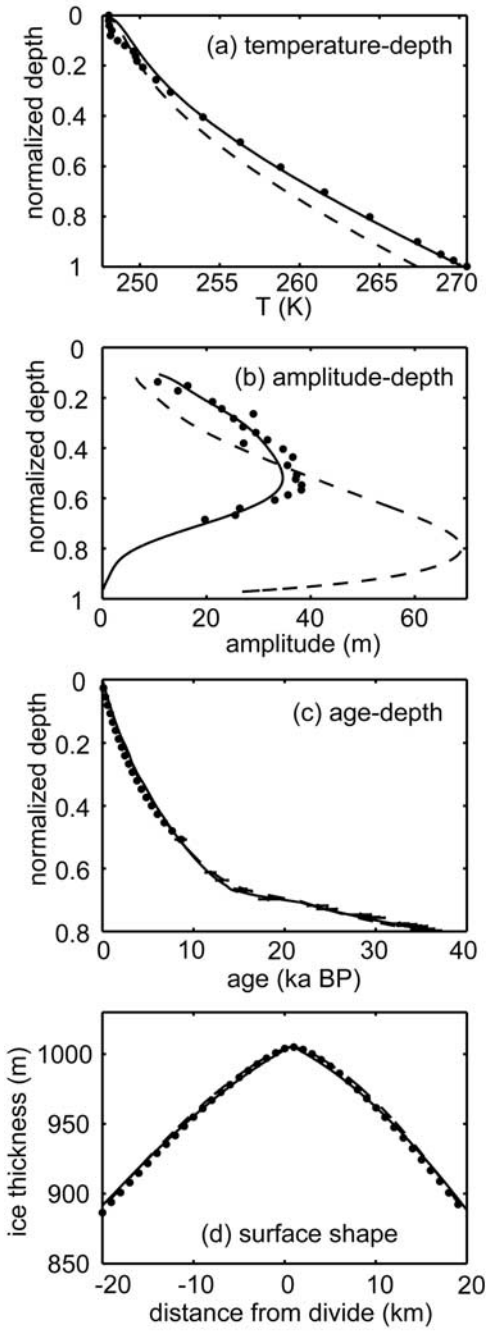

Figure 6. Modeled (curves) and observed (solid circles) variables at Siple Dome. Solid and dashed curves represent results from the favored and reference models, respectively. (a) Temperature profile, (b) bump amplitude profile observations limited to the depth range $0.1H$ to $0.7H$ (H is the ice thickness), (c) age-depth relationship, and (d) surface elevation.

the ice dynamics are specified constant (dashed curves); comparison with observations (solid circles in Figure 6) shows that the model-observation misfit is acceptable for the surface shape, less acceptable for the age-depth relationship, poor for the temperature profile, and poor for the bump amplitude profile. Ice dynamics must be included in the model in order to reduce the misfits.

[31] We reduce the number of model parameters by specifying northward divide migration starting 2.5 ka BP at a rate of 0.5 m a^{-1}, on the basis of work by *Nereson et al.* [1998b]. We then search for histories of ice thickness, the onset of divide flow, and divide scouring that provide an ''acceptable'' match to the measurements (solid black curves in Figure 6). Uncertainties associated with each of the measurements are used to determine what is an ''acceptable match.'' Specifically:

[32] 1. Age-depth relationship. Uncertainties in the observed age-depth relationship increase with depth and we use 1σ uncertainties given by *Taylor et al.* [2005] and *Brook et al.* [2005] to define the envelope of uncertainty shown in the age-depth misfit figures (e.g., Figure 7a). Although the goal is to match the observations to within 1σ uncertainty, model results are outside the envelope at several depths; model ages near the surface are generally too old because we do not account for the affects of firn densification. Matching ages in the lower $\sim$20% of the ice column is problematic and we do not attempt to match the ages older than 40 ka.

[33] 2. Temperature profile. We assume that the uncertainty in the modeled surface temperatures during the glacial is $\pm 2^{\circ}$C (see Appendix A), which would change the modeled, present-day temperature profile by about 0.5°C. We accept models that provide a match within 0.5°C of the measurements. Anomalous temperature measurements in the upper 200 m have been attributed to recent (past 1.5 ka) changes in surface temperature [*Engelhardt*, 2004]. However, there is no evidence for such changes in the proxy surface temperature record (A. Schilla, personal communication, 2007). Furthermore, the anomalous temperatures have not been detected in other temperature measurements in the area (G. Clow, personal communication, 2004). As such, we do not attempt to match the upper 200 m of the temperature profile (Figure 6a).

[34] 3. Bump amplitude profile. On the basis of uncertainties associated with picking the depth of radar-detected layers and defining the bump amplitude profile (Figure 6b), we accept a misfit of 5 m to the bump amplitude and 100 m to the depth of the bump amplitude maximum.

[35] 4. Surface shape. When fitting the surface shape (Figure 6d), we accept a misfit of 5 m. This is equivalent to a slope error of <5% of the mean, modern slope over the 20 km from the divide to the edge of the model domain.

[36] Histories that produce an acceptable match are:

[37] 1. Divide flow starting 3 ka BP and ongoing divide migration starting 2.5 ka BP.

[38] 2. Total thinning of 350 m from 15 ka to 14 ka BP.

[39] 3. Flow enhancement ($E \neq 1$) starting 30 ka BP and then evolving in space and time as described above.

[40] 4. Divide scouring at a rate of 2.5 mm a^{-1} starting 3 ka BP (coincident with the onset of divide flow) and continuing today.

5. Model Sensitivity

[41] A number of different histories of climate, ice thickness, onset of divide flow, flow enhancement, and divide scouring match the observations, but some can be eliminated because they are not compatible with all the observational data. Others can be rejected because they are

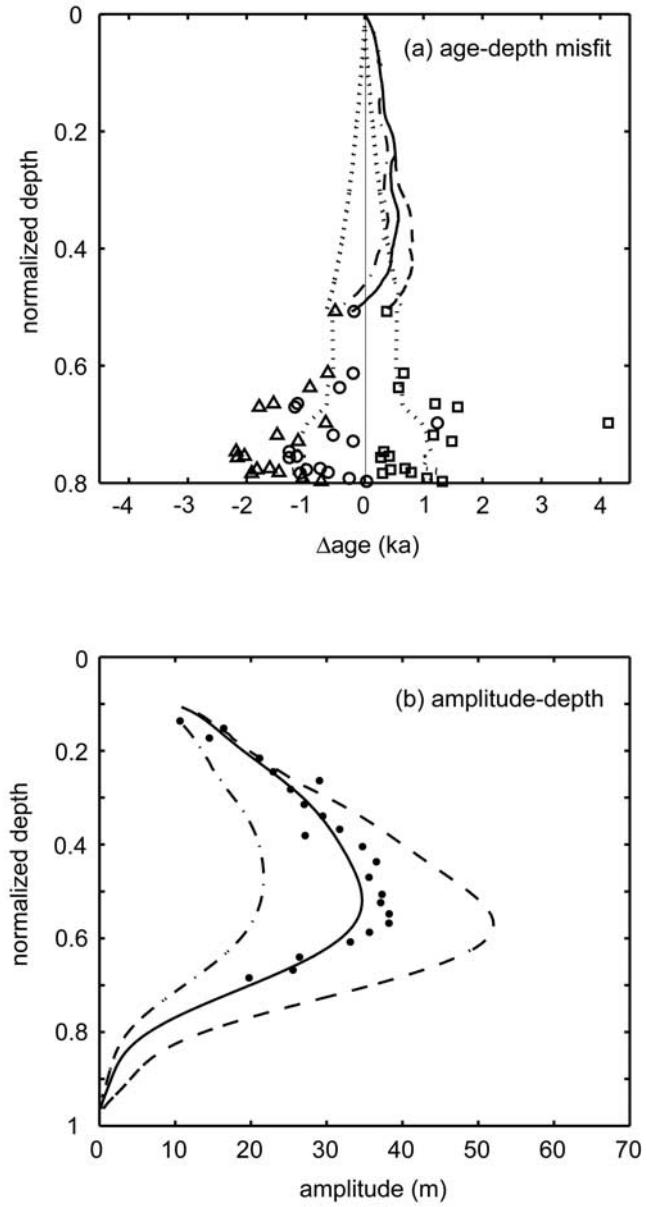

Figure 7. Model sensitivity to divide flow starting at 3 ka BP (favored time, solid curves and open circles), 1.5 ka BP (dash-dotted curves and triangles), and 6 ka BP (dashed lines and squares). (a) Misfit to age-depth relationship (model measurements). (b) Bump amplitude profile (measurements shown as solid circles).

physically unrealistic. Below we investigate the sensitivity to small perturbations to our favored histories of climate and ice dynamics.

5.1. History of Divide Location

[42] Figure 7 shows the misfit (model-observation) for the age-depth relationship, and the bump amplitude profile for our favored model (divide flow starting 3 ka BP); for divide flow starting 6 ka BP; and for divide flow starting 1.5 ka BP. In all cases, northward migration of the divide starts after 2.5 ka BP, and scouring of accumulation at the divide is coincident with divide flow. Misfits for the present-day surface shape and temperature profile are not shown because they are relatively insensitive to the onset of divide flow. Other things being equal, the age at a given depth beneath a divide becomes progressively older with increasing time after the onset of divide flow. Figure 7a shows that model ages at depth are too young (compared with measurements) for the case of divide flow starting 1.5 ka BP, and too old for divide flow starting 6 ka BP. Figure 7b shows that both the maximum amplitude of the bump and the depth of the maximum increase with increasing time after the onset of divide flow. Our favored timing for the onset of divide flow (3 ka BP) also depends on the evolution of ice flow enhancement, which we discuss below.

5.2. Ice Thickness History

[43] Ice sheet thinning affects the evolution of layers throughout the ice sheet. Other things being equal, the age at a given depth becomes progressively older with increased ice sheet thinning. Figure 8 shows misfits (model-observation) for the age-depth relationship, and for the temperature profile for our favored model (thinning of 350 m); for 250-m thinning; and for 450-m thinning between 15 ka and 14 ka BP. Misfits to the surface shape are not shown because thinning that occurred >700 yrs ago has minimal influence on the present-day surface profile. Similarly, we do not show misfits to the bump amplitude profile because the prescribed thinning ended long before the onset of divide flow.

[44] Thinning between 15 ka and 14 ka BP does not affect the age-depth relationship in ice younger than 14 ka BP (the upper 650 m) but for older ice, model ages for 250-m thinning are too young, while those for 450-m thinning are too old (Figure 8a). The basal temperature for the reference state (no thinning) is more than 3°C colder than observed (Figure 6a). Thicker ice in the past is more insulating and the misfit improves for models that include thick ice in the past. The basal ice is still too cold if we assume the ice sheet was just 250 m thicker in the past but the match improves if it was 450 m thicker (Figure 8b). However, the misfit to the age-depth relationship is less acceptable for 450 m of thinning (Figure 8a); thinning of 350 m is a reasonable compromise.

[45] Figure 9 shows misfits (model-observation) for the age-depth relationship, and for the temperature profile for our favored model (350-m thinning between 15 ka and 14 ka BP) and for 350-m thinning between 20–15 ka BP, 20–12 ka BP, 15–10 ka BP, 15–2 ka BP, and 7–2 ka BP. For thinning ending 2 ka BP, the modeled age-depth relationship is too old at all depths and the modeled temperature profile is much too cold at middepths (Figures 9a and 9b, pluses and asterisks); cold ice at mid depth, indicated by a reversal in the temperature misfit in Figure 9b, is not evident in the measurements (Figure 6a).

[46] For thinning ending before 10 ka BP, the fit to the temperature measurements is acceptable (Figure 9b). For thinning starting at 20 ka BP, however, the deep ice is too young (Figure 9a, squares and diamonds). The misfit to the age-depth relationship for our favored scenario (thinning from 15–14 ka BP, Figure 9a, open circles) is similar to that for thinning from 15–10 ka BP (Figure 9a, triangles), but only in the former case are all of the misfits less than, or very close to, the estimated 1σ age uncertainties.

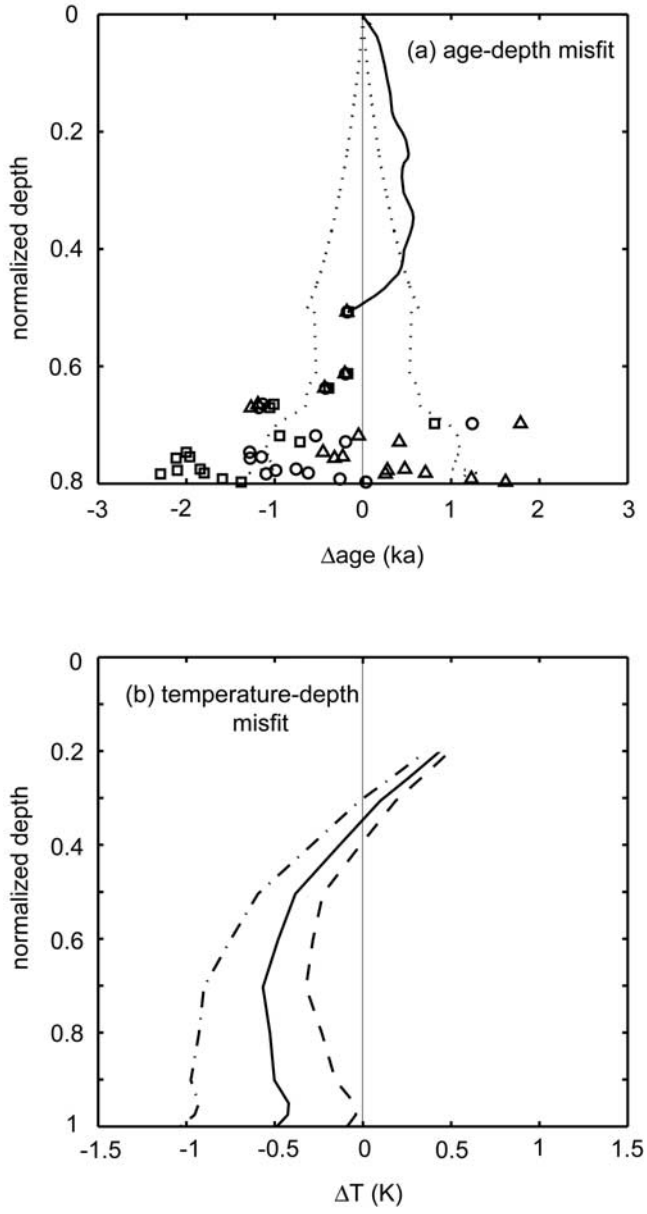

Figure 8. Model sensitivity to thinning of 350 m (favored amount, solid curves and open circles), 250 m (dash-dotted curves and squares), and 450 m (dashed curves and triangles) between 15 ka and 14 ka BP. (a) Misfit to age-depth relationship. Thinning between 15 ka and 14 ka BP does not affect the age-depth relationship in ice younger than 14 ka BP (the upper 650 m), hence the overlap of line types. We do not attempt to match ages in the lower 20% of the ice sheet (see section 4). (b) Misfit to temperature profile. We do not attempt to match temperature measurements in the upper 20% of the ice sheet (see section 4).

5.3. Evolution of Ice Fabric and Flow Enhancement

[47] Figure 10 shows misfits (model-observation) for our favored model (based on Figure 5); for no enhancement anywhere ($E(x, z, t) = 1$); for no enhancement in the upper column, but a layer of stiff ice near the bed (a "false bed"); and for 50% greater contrast between E_c and E_s in the upper layer (to approximate the effects of a more tightly focused *c* axis fabric).

[48] Assuming no enhancement yields a poor match to observations: the temperature profile is too cold (Figure 10a, dashed curve); matching the magnitude of the bump amplitude requires the onset of divide flow to be much more than 3 ka BP, but matching the depth of the amplitude maximum requires the onset of divide flow to be less than 3 ka BP (Figure 10b, dashed curve); the modeled age at depth is too young (Figure 10c, dotted curve and squares). Invoking

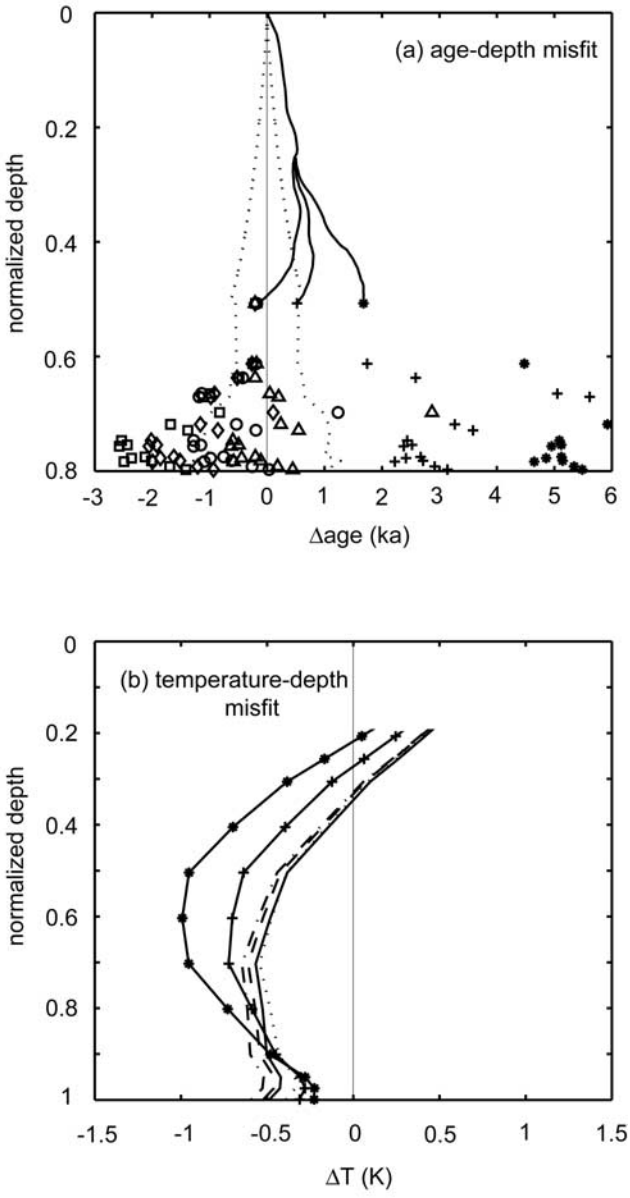

Figure 9. Model sensitivity to 350 m of thinning from 15–14 ka BP (favored timing, solid curves and open circles), 20–15 ka BP (dash-dotted curves and squares), 20–12 ka BP (dashed curves and diamonds), 15–10 ka BP (dotted curves and triangles), 15–2 ka BP (solid curves and pluses), and 7–2 ka BP (solid curves and asterisks). (a) Misfit to age-depth relationship. (b) Misfit to temperature profile.

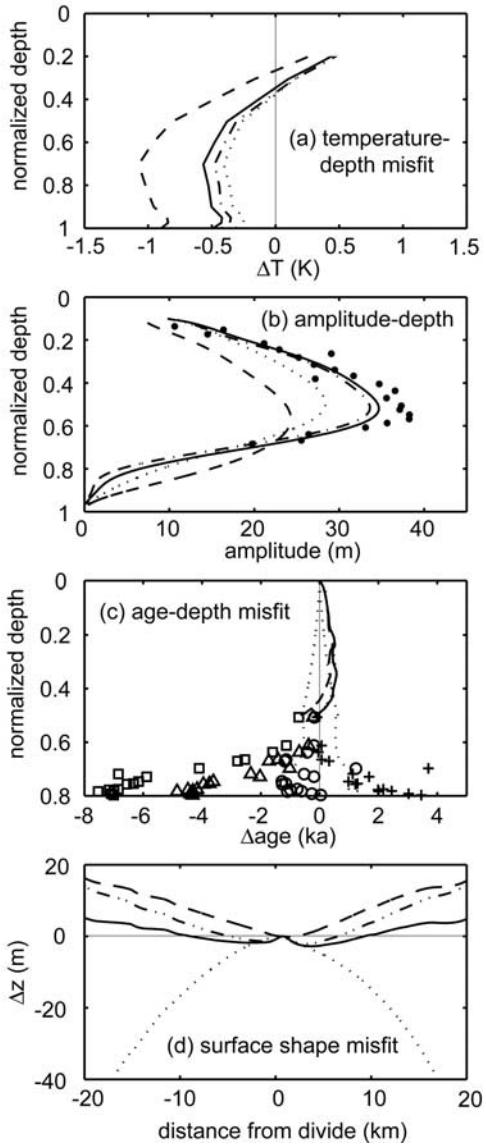

Figure 10. Model sensitivity to flow enhancement: favored distribution shown in Figure 5 (solid curves and open circles), $E = 1$ everywhere (dashed curves and squares), stiff basal layer only (dotted curves and triangles), and increased orientation (''stronger'') fabric (dash-dotted curves and crosses). (a) Misfit to temperature profile. (b) Bump amplitude profile (measurements shown as solid circles). (c) Misfit to age-depth relationship. (d) Misfit to surface shape.

more thinning would reduce the misfit to the age-depth relationship and to the temperature profile, but not to the bump amplitude profile. Including a layer of stiff ice near the bed in the model reduces the mismatch to the temperature profile (Figure 10a, dotted curve), and shifts the bump amplitude profile upward (Figure 10b, dotted curve). The mismatch in age at depth is also decreased, although the modeled age at depth is still too young (Figure 10c, triangles). Including only the stiff layer results in a surface profile that is much too steep (Figure 10d, dotted curve). Our favored model (Figure 10, solid curves and circles) improves the fit to all observations. Increasing the contrast between E_c and E_s by 50%, to simulate a tighter c axis fabric, has a small effect on the model mismatch to the measured temperature and bump amplitude profiles (Figures 10a and 10b, dash-dotted curve). The age, however, is too old at depth (Figure 10c, pluses), and the surface shape is too shallow (Figure 10d, dash-dotted curve).

[49] We examine the sensitivity to the evolution of E by varying the ''start'' time (when fabric first starts to evolve) and the ''end'' time (when E reaches the ''modern'' values shown in Figure 3). Figure 11 shows our favored model

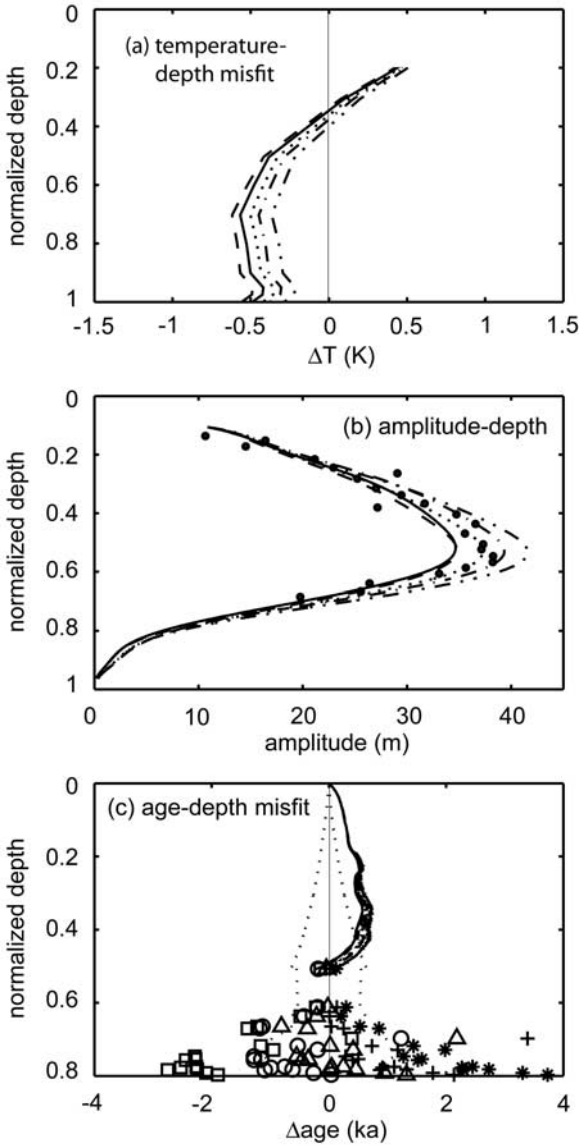

Figure 11. Model sensitivity to flow enhancement starting at 30 ka BP (favored timing, solid curves and open circles), starting at 20 ka BP (dashed curves and squares), starting at 40 ka BP (dotted lines and triangles), starting at 30 ka BP and ending at 5 ka BP (dash-dotted curves and crosses), and starting at 30 ka BP and ending at 10 ka BP (dash-double-dotted curves and asterisks). (a) Misfit to temperature profile. (b) Bump amplitude profile (measurements shown as solid circles). (c) Misfit to age-depth relationship.

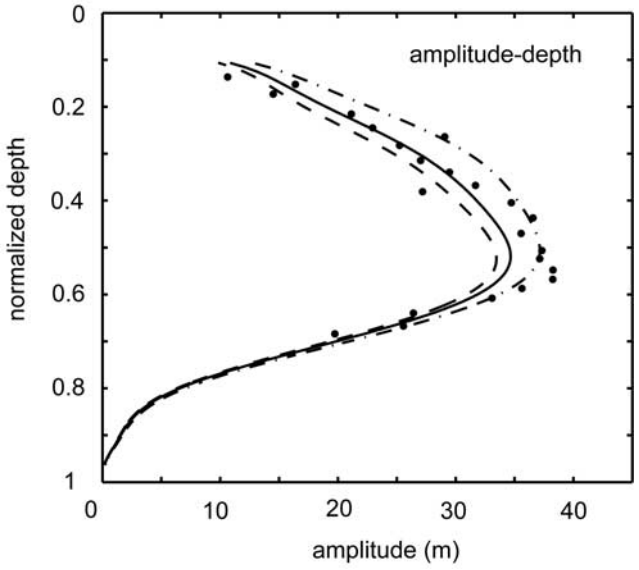

Figure 12. Model sensitivity of bump amplitude profile to divide scouring of 2.5 mm a^{-1} (favored value, solid line), 1.2 mm a^{-1} (dashed curve), and 5 mm a^{-1} (dash-dotted curve). Measurements are shown as solid circles.

(fabric evolution starting 30 ka BP), and results for cases where the start time is changed by ±10 ka. Also shown are results for cases where the end time is changed from its favored value (today) to 5 ka and 10 ka BP. Cases where enhancement has been active for longer require less thinning to match the age-depth relationship because we assume a flank flow regime prior to the onset of divide flow, and oriented fabric is "soft" to surface-parallel shear on the flanks. Stiff basal ice inhibits the vertical advection of cold surface ice, so that if enhancement is active for longer, the ice column is warmer than if enhancement is active for a short time or not at all. At Siple Dome, however, this effect is small compared to the effects of thickness changes.

5.4. History of Divide Scouring

[50] Figure 12 shows our favored model (divide scouring of 2.5 mm a^{-1} when the divide is in place) and results for scouring of 1.2 and 5.0 mm a^{-1}. Misfits for the age-depth relationship, the temperature profile, and the present-day surface shape are not shown because they are insensitive to such small amounts of scouring (less than 5% of the accumulation rate during the last 3 ka). Although the effects of scouring are small, increased local scouring at the divide effectively increases the bump amplitude, and shifts the position of the maximum bump amplitude closer to the surface (Figure 12) (as shown previously by *Nereson and Waddington* [2002]).

5.5. Accumulation Rate History

[51] *Spencer* [2005] estimated a 2σ uncertainty of 26% for his accumulation rate history and noted that independent estimates of accumulation rate through the Holocene at Siple Dome are within 10% of his values. Figure 13 shows the effects of changing the Spencer accumulation rate history by ± 10% of its mean value during the Holocene.

[52] Higher annual accumulation produces thicker annual layers; a given depth interval contains fewer layers making the age-depth relationship relatively young (Figure 13c, dashed curve and squares). To compensate, more strain thinning of layers is needed to match the observed age-

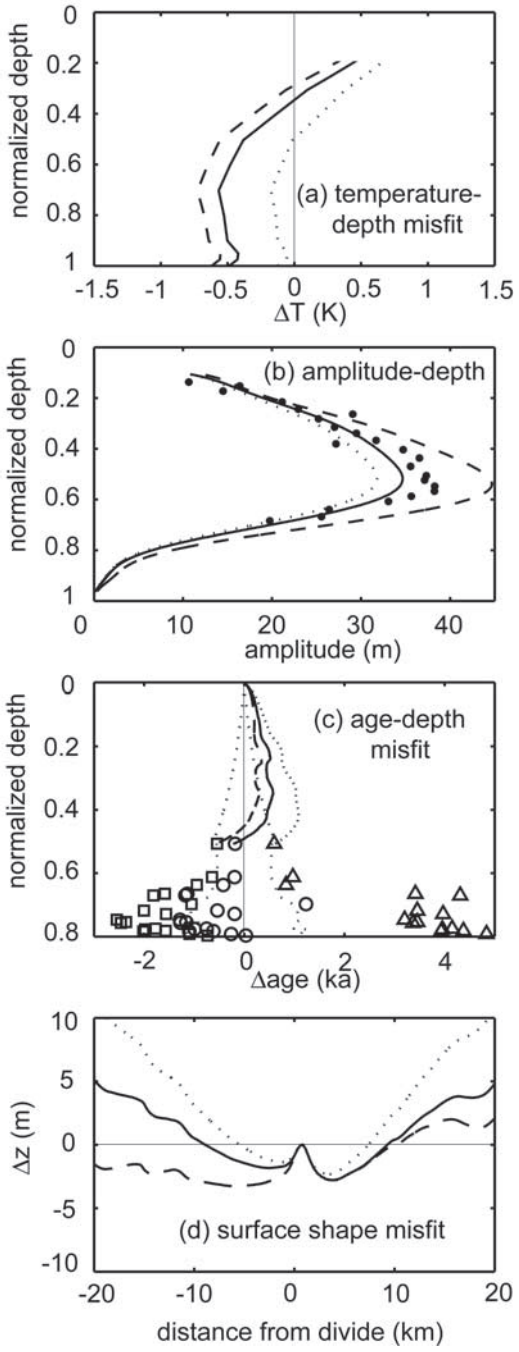

Figure 13. Model sensitivity to the accumulation rate history: favored history shown in Figure 2a (solid curves and open circles), favored plus 0.01 m a^{-1} (dashed curves and squares), and favored minus 0.01 m a^{-1} (dotted curves and triangles). (a) Misfit to temperature profile. (b) Bump amplitude profile (measurements shown as solid circles). (c) Misfit to age-depth relationship. (d) Misfit to surface shape.

depth relationship (the opposite is true for decreased accumulation). Increased vertical advection associated with increased accumulation results in a temperature profile that is relatively cold (Figure 13a) and increased thinning (needed to match the age-depth relationship) would further increase the temperature misfit. Higher accumulation rates also require relatively higher mass flux to maintain steady state and thus faster horizontal velocities. In turn, faster velocities imply steeper surface slopes (necessary to increase the driving stress. Figure 13d, dashed curve). Further, relatively fast horizontal velocities increase the contrast between divide flow and flank flow regimes and the amplitude of the divide bump increases slightly (Figure 13b). The effect on the depth of the amplitude maximum is small however.

[53] We have also examined the effects of randomly perturbing the accumulation rate history by ± 10%. Such perturbations generally have a minor effect on the misfits to observations. One exception is during the period of low accumulation (0.04 ma^{-1}, Figure 2a) at the LGM (coinciding with a depth of ~700 m); under these conditions a perturbation in the accumulation rate has a large effect on the age of a layer.

6. Discussion

[54] Multiple combinations of past climate, ice thickness, ice divide position and ice fabric can produce the same age-depth relationship observed in an ice sheet today. Our study shows how additional measurements (internal stratigraphy, depth profiles of temperature, ice fabric and texture) can be used to help constrain the histories of climate and ice dynamics. Specifically, the temperature measurements at Siple Dome provide a strong constraint on the magnitude and timing of thinning; thicker ice in the past is needed to match the basal temperature, but much thicker ice requires more thinning (to reach the present-day thickness), resulting in cold ice at mid depths. Such a "bow" in the temperature profile might also be caused by recent thinning. At Siple Dome during the Holocene, ice thickness $H \approx 1000$ m, accumulation rate $\dot{b} \approx 0.1$ m a^{-1}, and the characteristic timescale for heat advection, $\tau = H/\dot{b}$, is ~10 ka. Anomalously cold ice at middepths is not evident in the measurements (Figure 6a), which is consistent with moderate thinning ending more than 10 ka BP.

[55] The pattern of internal layers beneath the divide provides a constraint on the timing of onset of divide flow. Knowledge of the divide history is important because other things being equal, the age-depth relationship observed today is strongly dependent on the histories of thinning and divide location. Compared to the case of no thinning, relatively old layers at depth might arise from ice sheet thinning or because a divide was present for a long period of time. Analysis of the bump amplitude profile at Siple Dome indicates that the onset of divide flow was relatively recent (3 ka BP). In this case, matching the observed age-depth relationship at Siple Dome requires thinning.

[56] Some ice flow enhancement is needed to match the observed bump amplitude profile (Figure 10). The bump amplitude profile trends toward zero several hundred meters above the bed. The simplest explanation for this pattern is to invoke a layer of stiff ice that effectively causes a "false bed". This stratigraphy, stiff ice near the bed overlain by a layer that deforms more easily in shear, has also been inferred in model studies of ice stream tributaries near Byrd Station [*Wang et al.*, 2003]. Flow modeling constrained by ice core measurements [*Wang and Warner*, 1999] and observations using polarized, ice-penetrating radar [*Fujita et al.*, 1999] indicate that this combination of basal layers may also be widespread in East Antarctica. Improved understanding of the evolution of ice fabric and texture, and their influence on ice flow (and hence the age-depth relationship, the temperature profile as well as the bump amplitude profile. See Figure 10) is needed to improve predictive models of ice sheet behavior.

[57] The magnitude of our favored thickness change (about 350 m since the LGM) is within the range inferred by *Waddington et al.* [2005], but is about half that required by the reconstruction of *Denton and Hughes* [2002]. Constraints from the measured temperature profile and the age-depth profile indicate that most thinning took place late in the Pleistocene, most likely from 15–14 ka BP but possibly from 15–10 ka BP. These findings are consistent with stable isotope profiles from Byrd and Siple Dome. A. Schilla (personal communication, 2007) attributes differences in the profiles to relative elevation changes; assuming that the elevation at Byrd did not change suggests that Siple Dome thinned about 200 m between 20 and 12 ka BP. Although our favored time of thinning is earlier than that inferred from geologic evidence from the western margin of the Ross Sea Embayment and glaciological evidence from Roosevelt Island [*Conway et al.*, 1999], it does not preclude later thinning around the margins.

[58] It is probable that Siple Dome thinned in response to acceleration and thinning of the surrounding ice streams. Model experiments of *Parizek et al.* [2003] indicate that the ice streams probably slowed down during the glacial period but did not stop entirely. They also showed that increased flow rates, in response to postglacial warming, would likely be delayed until some time after 13 ka BP. Increased activity of the ice streams could also be forced by changes near the grounding line. Observations of the Amundsen Sea Sector of West Antarctica show that the effects of changing conditions near the grounding line of ice streams propagate rapidly (less than 20 years) more than 100 km upstream [*Joughin et al.*, 2003; *Rignot*, 2002; *Shepherd et al.*, 2001]. These observations have been mimicked in model experiments; *Payne et al.* [2004] showed that relatively small perturbations to the basal shear stress near the grounding line of Pine Island Glacier can propagate several hundred kilometers upstream over decadal timescales.

[59] Our favored timing of thinning (between 15 k and 14 ka BP) is coincident with meltwater pulse 1A [*Fairbanks*, 1989] at ~14.5 ka BP, a 20 m rise in sea level that took place over several hundred years. This large, rapid rise in sea level would force ice near the grounding line to float and would remove basal resistance there entirely. The resulting thinning and flow acceleration would propagate upstream over time and would do so more rapidly along streaming than nonstreaming ice. Along ice streams, additional feedbacks between evolving stresses in the ice and basal conditions could also lead to relatively faster inland propagation and/or longer propagation distances [*Price et al.*, 2005]. Although it is possible that thinning in the

central Ross Sea Embayment contributed to meltwater pulse 1A, its total contribution to global sea level rise would have been less than 2 m.

7. Conclusions

[60] Ice flow modeling, constrained by multiple data sets, provides a way to help unravel the history of an ice sheet. As in previous work [e.g., *Waddington et al.*, 2005], we use a measured age-depth relationship to constrain histories of thickness and divide flow at Siple Dome. We also show that the measured temperature-depth profile helps to constrain the magnitude and timing of thinning and that the internal stratigraphy helps to constrain the timing of the onset of divide flow. The latter is important for separating the competing effects of ice thickness change and divide flow history on the observed age-depth relationship. Results also indicate that ice fabric and texture have important effects on the flow field; improved understanding of the evolution of ice fabric and texture, and its influence on ice flow, is needed to improve predictive models of ice sheet behavior.

[61] Our favored reconstruction points to 350 m of thinning at Siple Dome between 15 and 14 ka BP. This timing is coincident with the time of meltwater pulse 1A, when global sea level increased by more than 20 m in a few hundred years. We speculate that increased activity of the surrounding ice streams forced by rapid sea level rise may have initiated thinning of Siple Dome during the late Pleistocene.

Appendix A: Uncertainty in Modeled Temperatures

[62] Surface temperatures T_S (t) at time t in the past are calculated using the age-depth relationship and measurements of stable isotope changes along the ice core (A. Schilla, personal communication, 2007). Differences from the present-day surface temperature, T_S (0), are assumed to be related to differences in Deuterium stable isotope ratios according to

$$T_S(t) - T_S(0) = \alpha[\delta D(t) - \delta D(0)] + \beta, \qquad \text{(A1)}$$

where $\alpha = \partial T/\partial \delta D$, and β accounts for second-order corrections to the temperature change (e.g., changes in isotopic concentration at the precipitation source). The value for α for a region is calculated from modern-day observations and is generally treated as a constant but in reality, α varies spatially and temporally [*Kavanaugh and Cuffey*, 2003]. *Cuffey et al.* [1994] estimated that α changed by a factor of 2 across the glacial-interglacial transition in central Greenland, while *Jouzel et al.* [2003] suggested that uncertainty of 10–20% is expected when extrapolating values back in time.

[63] The surface temperature history of A. Schilla (personal communication, 2007) is well approximated (to within a fraction of a degree) by setting $\alpha = 5.52$ ($= 8 \times 1.45^{-1}$) and $\beta = 0$ in equation (A1). A 20% uncertainty in α translates to about 2°C uncertainty in the reconstructed surface temperatures, which changes the modeled temperature profile by about ±0.5°C. Misfits within 0.5°C are considered acceptable.

Appendix B: Treatment of Transitional Flow at an Ice Divide

[64] We simulate the transition from a flank to a divide through a small modification of the layer-tracking submodel but no change to the flow model itself. The flow model assumes that a divide exists near the present-day core site at all times. To simulate conditions prior to the onset of divide flow, we replace the modeled layer shapes in the divide region (within a distance of about ±5 ice thicknesses from the divide) by a spline fit to the layer shapes outside of this region; the layer-tracking submodel treats layers beneath the divide as if they experienced flank flow rather than divide flow. The age-depth relationship for this "false" flank is identical to that for a true flank site. After the onset of divide flow, this constraint is removed and new and preexisting layers are everywhere advected through the flow field. This simplification biases the model temperature field to be too warm, because it assumes that a divide has always been in place. In steady state under modern conditions, however, the maximum difference between temperatures beneath the divide at Siple Dome and at a flank site of similar thickness is ~0.5°C. This is similar to the uncertainty associated with matching the observed temperature profile (Appendix A). Thus the consequence of this simplification is within our tolerance for matching the temperature measurements.

[65] We force divide migration late in the model run by increasing the mass flux at one lateral boundary and decreasing it by an equal amount at the opposite boundary. The change in flux needed for a desired rate of migration is found through experiments. Changing of the boundary fluxes causes the velocity field itself to change so that there are no additional uncertainties introduced into the model temperature field.

[66] **Acknowledgments.** We thank Matt Spencer and Richard Alley for the accumulation rate history and Annie Schilla and Jim White for the surface temperature history. We thank these same people as well as Christina Hulbe, Tom Neumann, and Charlie Raymond for many constructive discussions. Two anonymous reviewers made suggestions that also helped to improve the manuscript. Christina Hulbe and Michael Price provided CPU time. This work was supported by NSF grants OPP-0125610 and OPP-0087345.

References

Anderson, J., S. Shipp, A. Lowe, J. Wellner, and A. Mosola (2002), The Antarctic ice sheet during the Last Glacial Maximum and its subsequent retreat history: A review, *Quat. Sci. Rev.*, *21*, 49–70.

Brook, E., J. White, A. Schilla, M. Bender, B. Barnett, J. Severinghaus, K. Taylor, R. Alley, and E. Steig (2005), Timing of millennial-scale climate change at Siple Dome, West Antarctica, during the last glacial period, *Quat. Sci. Rev.*, *24*, 1333–1343.

Conway, H., B. Hall, G. Denton, A. Gades, and E. Waddington (1999), Past and future grounding-line retreat of the West Antarctic Ice Sheet, *Science*, *286*(5438), 280–283.

Cuffey, K., R. Alley, P. Grootes, J. Bolzan, and S. Anandakrishnan (1994), Calibration of the δ^{18}O isotopic paleothermometer for central Greenland, using borehole temperatures, *J. Glaciol.*, *40*, 341–349.

Dahl-Jensen, D. (1989), Steady thermomechanical flow along two-dimensional flow lines in large grounded ice sheets, *J. Geophys. Res.*, *94*(B8), 10,355–10,362.

Denton, G., and T. Hughes (2002), Reconstructing the Antarctic Ice Sheet at the Last Glacial Maximum, *Quat. Sci. Rev.*, *21*, 193–202.

Denton, G., M. Prentice, and L. Burckle (1991), Cainozoic history of the Antarctic Ice Sheet, in *The Geology of Antarctica*, edited by J. Tingey, pp. 365–433, Clarendon, Oxford, U. K.

DiPrinzio, C., L. Wilen, R. Alley, J. Fitzpatrick, M. Spencer, and A. Gow (2005), Fabric and texture at Siple Dome, Antarctica, *J. Glaciol.*, *51*, 281–290.

Engelhardt, H. (2004), Ice temperature and high geothermal flux at Siple Dome, West Antarctica, from borehole measurements, *J. Glaciol.*, *50*, 251–256.

Fairbanks, R. (1989), A 17,000-year glacio-eustatic sea level record: Influence of glacial melting rates on the Younger Dryas event and deep-ocean circulation, *Nature*, *232*(637), 637–742.

Fujita, S., H. Maeno, S. Uratsuka, S. Furukawa, S. Mae, Y. Fujii, and O. Watanabe (1999), Nature of radio echo layering in the Antarctic ice sheet detected by a two-frequency experiment, *J. Geophys. Res.*, *104*(B6), 13,013–13,024.

Hamilton, G. (2002), Mass balance and accumulation rate across Siple Dome, West Antarctica, *Ann. Glaciol.*, *35*, 102–106.

Hawley, R., E. Waddington, G. Lamorey, and K. Taylor (2004), Vertical-strain measurements in firn at Siple Dome, Antarctica, *J. Glaciol.*, *50*, 447–452.

Huybrechts, P. (2002), Sea-level changes at the LGM from ice-dynamics reconstructions of the Greenland and Antarctic ice sheets during the glacial cycles, *Quat. Sci. Rev.*, *21*, 203–231.

Jacobel, R., T. Scambos, C. Raymond, and A. Gades (1996), Changes in the configuration of ice stream flow from the West Antarctic ice sheet, *J. Geophys. Res.*, *101*(B3), 5499–5504.

Joughin, I., E. Rignot, C. E. Rosanova, B. K. Lucchitta, and J. Bohlander (2003), Timing of recent accelerations of Pine Island Glacier, Antarctica, *Geophys. Res. Lett.*, *30*(13), 1706, doi:10.1029/2003GL017609.

Jouzel, J., F. Vimeux, N. Caillon, G. Delaygue, G. Hoffmann, V. Masson-Delmotte, and F. Parrenin (2003), Magnitude of isotope/temperature scaling for interpretation of central Antarctic ice cores, *J. Geophys. Res.*, *108*(D12), 4361, doi:10.1029/2002JD002677.

Kavanaugh, J. L., and K. M. Cuffey (2003), Space and time variation of δ^{18}O and δD in Antarctic precipitation revisited, *Global Biogeochem. Cycles*, *17*(1), 1017, doi:10.1029/2002GB001910.

Nereson, N., and E. Waddington (2002), Isochrons and isotherms beneath migrating ice divides, *J. Glaciol.*, *48*, 95–108.

Nereson, N., R. Hindmarsh, and C. Raymond (1998a), Sensitivity of the divide position at Siple Dome, West Antarctica, to boundary forcing, *Ann. Glaciol.*, *27*, 207–214.

Nereson, N., C. Raymond, E. Waddington, and R. Jacobel (1998b), Migration of the Siple Dome Ice Divide, West Antarctica, *J. Glaciol.*, *44*, 643–652.

Nereson, N., C. Raymond, R. Jacobel, and E. Waddington (2000), The accumulation pattern across Siple Dome, West Antarctica, inferred from radar-detected internal layers, *J. Glaciol.*, *46*, 75–86.

Parizek, B., and R. Alley (2004), Ice-thickness and isostatic imbalances in the Ross Embayment, West Antarctica: Model results, *Global Planet. Change*, *42*, 265–278.

Parizek, B., R. Alley, and C. Hulbe (2003), Subglacial thermal balance permits ongoing grounding line retreat along the Siple Coast of West Antarctica, *Ann. Glaciol.*, *36*, 251–256.

Paterson, W. (1994), *The Physics of Glaciers*, p.14, Elsevier Sci., Oxford, U. K.

Paterson, W., and E. Waddington (1986), Estimated basal temperatures at Crete, Greenland, throughout a glacial cycle, *Cold Reg. Sci. Technol.*, *12*, 99–102.

Payne, A. J., A. Vieli, A. P. Shepherd, D. J. Wingham, and E. Rignot (2004), Recent dramatic thinning of largest West Antarctic ice stream triggered by oceans, *Geophys. Res. Lett.*, *31*, L23401, doi:10.1029/2004GL021284.

Pettit, E. (2003), Unique dynamic behaviors of ice divides: Siple Dome and the rheological properties of ice, Ph.D. dissertation, Univ. of Wash., Seattle.

Price, S., H. Conway, E. Waddington, and R. Bindschadler (2005), Investigating feedbacks between basal sliding, frictional melting, and longitudinal-stress transmission, *Eos Trans. AGU*, *86*(52), Fall Meet. Suppl., Abstract C44A-06.

Price, S. F., E. D. Waddington, and H. Conway (2007), A full-stress, thermomechanical flow band model using the finite volume method, *J. Geophys. Res.*, *112*, F03020, doi:10.1029/2006JF000724.

Raymond, C. (1983), Deformation in the vicinity of divides, *J. Glaciol.*, *34*, 357–373.

Raymond, C., N. Nereson, A. Gades, H. Conway, R. Jacobel, and T. Scambos (1995), Geometry and stratigraphy of Siple Dome, Antarctica, *Antarct. J. U.S.*, *30*(5), 91–93.

Rignot, E. (2002), Ice-shelf changes in Pine Island Bay, Antarctica, *J. Glaciol.*, *48*, 247–256.

Shepherd, A., D. Wingham, J. Mansley, and H. Corr (2001), Inland thinning of Pine Island Glacier, West Antarctica, *Science*, *291*, 862–864.

Spencer, M. (2005), Understanding paleoclimate change through firnification modeling, Ph.D. dissertation, Pa. State Univ., Univ. Park.

Steig, E., J. Fastook, C. Zweck, I. Goodwin, K. Licht, J. White, and R. Ackert (2001), West Antarctic ice sheet elevation changes, in *The West Antarctic Ice Sheet: Behavior and Environment*, *Antarct. Res. Series.*, vol. 77, edited by R. Alley and R. Bindschadler, pp. 75–90, AGU, Washington, D. C.

Stone, J., G. Balco, D. Sugden, M. Caffee, L. Sass III, S. Cowdery, and C. Siddoway (2003), Holocene deglaciation of Marie Byrd Land, West Antarctica, *Science*, *299*(5603), 99–102.

Taylor, K., et al. (2005), Dating the Siple Dome (Antarctica) ice core by manual and computer interpretation of annual layering, *J. Glaciol.*, *50*, 453–461.

Vaughan, D., H. Corr, C. Doake, and E. Waddington (1999), Distortion of isochronous layers in ice revealed by ground-penetrating radar, *Nature*, *398*(6725), 323–326.

Waddington, E., H. Conway, E. Steig, R. Alley, E. Brook, K. Taylor, and J. White (2005), Decoding the dipstick: Thickness of SDM, West Antarctica, at the Last Glacial Maximum, *Geology*, *33*(4), 281–284.

Wang, W., and R. Warner (1999), Modelling of anisotropic ice flow in Law Dome, East Antarctica, *Ann. Glaciol.*, *29*, 184–190.

Wang, W., H. Zwally, C. Hulbe, M. Siegert, and I. Joughin (2003), Anisotropic ice flow leading to the onset of Ice Stream D, West Antarctica: Numerical modeling based on the observations from Byrd Station borehole, *Ann. Glaciol.*, *39*, 397–403.

Zumberge, M., D. Elsberg, W. Harrison, E. Husmann, J. Morack, E. Pettit, and E. Waddington (2002), Measurement of vertical strain rate and velocity at Siple Dome, Antarctica, with optical sensors, *J. Glaciol.*, *48*, 217–225.

H. Conway and E. D. Waddington, Department of Earth and Space Sciences, University of Washington, Seattle, WA 98195, USA.

S. F. Price, Bristol Glaciology Centre, School of Geographical Sciences, University of Bristol, Bristol BS8 1SS, UK. (s.f.price@bristol.ac.uk)